Investigation of the factors contributing to skin friction coefficient in adverse pressure gradient turbulent boundary layer flow using direct numerical simulation

S. Senthil[1], C. Atkinson[1], V. Kitsios[2,1], A. Sekimoto[3,1] and J. Soria[1]

[1]Laboratory for Turbulence Research in Aerospace and Combustion,
Department of Mechanical and Aerospace Engineering, Monash University, Melbourne 3800, Australia

[2]CSIRO Oceans and Atmosphere, Castray Esplanade, Battery Point, Tasmania 7004, Australia

[3]Department of Materials Engineering Science, Osaka University, Osaka 560-8531, Japan

Abstract

Adverse pressure gradient (APG) turbulent boundary layers (TBLs) are found when the flow takes place over the diverging part of curved surfaces, like flow over the leeward side of an aerofoil section. This paper reports on a study of the various factors contributing to the skin friction coefficient in such flows. Specifically, it deals with the contributions to the wall shear stress from Reynolds stress, viscous effects and pressure gradient in an incompressible turbulent boundary layer flow. The skin friction coefficient is expressed in terms of the decomposition suggested by Renard & Deck [6] for boundary layer flows.

Numerical details

Direct numerical simulations (DNS) are performed to solve the incompressible Navier-Stokes equation for the primitive variables of pressure and velocity in Cartesian coordinates. The computational domain is a rectangular box with a no slip boundary condition at the lower wall. The APG is generated in the domain by specifying the wall normal velocity in the far-field (upper wall) where the spanwise vorticity is zero. The inflow boundary condition is obtained by recycling and mapping a cross-plane from a downstream position [3, 4]. Periodic boundary conditions are applied in the spanwise direction while the outflow is a convective boundary condition [4]. The density (set to one) and kinematic viscosity are taken as constants. The reference velocity (U_e), displacement thickness (δ_1) and the momentum thickness (δ_2) are defined as follows [8, 4].

$$U_e(x) = U_\Omega(x, y_\Omega) \tag{1}$$

$$U_\Omega(x, y) = -\int_0^y \langle \Omega_z \rangle (x, \tilde{y}) \, d\tilde{y} \tag{2}$$

$$\delta_1(x) = \frac{-1}{U_e} \int_0^{y_\Omega} y \langle \Omega_z \rangle (x, y) dy \tag{3}$$

$$\delta_2(x) = \frac{-2}{U_e^2} \int_0^{y_\Omega} y U_\Omega \langle \Omega_z \rangle (x, y) dy - \delta_1(x) \tag{4}$$

where $\langle \Omega_z \rangle$ is the mean spanwise vorticity and y_Ω is the wall normal position at which the mean spanwise vorticity is 0.2% of the mean vorticity at the wall.

The non-dimensional pressure gradient (β) is defined as

$$\beta = \delta_1 \frac{P_{e,x}}{\tau_w} \tag{5}$$

for a unit density, where δ_1 is the displacement thickness, $P_{e,x}$ is the far-field pressure gradient and τ_w is the mean wall shear stress. In the domain of interest (DoI), $\beta = 39$ and the flow is
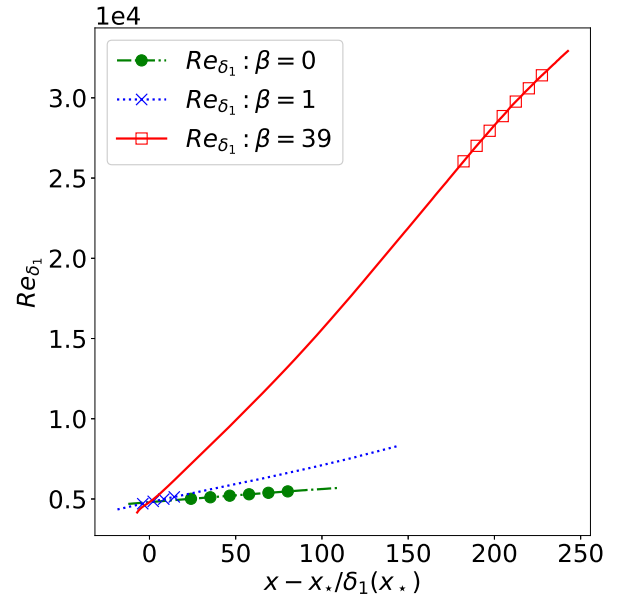
Figure 1: Re_{δ_1} for each case of β and their respective DoI is highlighted with the markers. $x_\star$ is the streamwise position where $Re_{\delta_1} = 4800$.

self-similar [4]. Within the DoI, the Reynolds number based on displacement thickness (Re_{δ_1}) varies from 22,200 to 28,800. When $\beta = 39$, the flow can be characterized as being at the verge of separation.

The analysis of the factors contributing to C_f is studied in boundary layer flows with three different pressure gradients in their respective DoI: $\beta=0$ (ZPG), $\beta=1$ (mild APG) and $\beta=39$ (strong APG). The number of grid points in the streamwise direction for each case in their respective DoI is given as follows: ZPG - 1035, mild APG - 582 and strong APG - 1001. Re_{δ_1} for all cases of β are shown in Figure 1 and the DoI for each case is highlighted with the markers. $x_\star$ is the streamwise position at which $Re_{\delta_1} = 4800$. $\delta_1(x_\star)$ is the displacement thickness at $x_\star$ [4].

The code uses hybrid OpenMP (Open Multi-Processing) and MPI (Message Passing Interface) parallelisation technique to decompose the domain. More detail of the code can be found in [7, 1]. The details of the far-field APG boundary condition and the numerical details of the simulations are described in [4].

Decomposition of skin friction coefficient (C_f)

Energy dissipation occurs whenever there is a relative motion between a fluid and an immersed object or when a fluid is transported in pipes. The major part of this energy dissipation is due to the presence of frictional drag in the TBL. It is important to undertstand the factors contributing to the friction drag and C_f. Renard & Deck introduced a theoretical decomposition for mean skin friction generation in a zero pressure gradient (ZPG) boundary layer flow. They presented the skin friction generated in both laminar and turbulent flows. The formulation (hereafter referred as Renard's formulation) is based on mean kinetic energy budget in the streamwise direction and is given as follows [6].

$$C_f = C_{f_a} + C_{f_b} + C_{f_c} \tag{6}$$

$$C_{f_a} = \frac{2}{U_e^3} \int_0^\infty \nu \left(\frac{\partial \langle u \rangle}{\partial y} \right)^2 dy \tag{7}$$

$$C_{f_b} = \frac{2}{U_e^3} \int_0^\infty -\langle u'v' \rangle \frac{\partial \langle u \rangle}{\partial y} dy \tag{8}$$

$$C_{f_c} = \frac{2}{U_e^3} \int_0^\infty (\langle u \rangle - U_e) \frac{\partial}{\partial y} \left(\frac{\tau}{\rho} \right) dy \tag{9}$$

where $\tau/\rho = \nu(\partial \langle u \rangle / \partial y) - \langle u'v' \rangle$.

The analysis is performed from an absolute reference frame which travels with the undisturbed fluid and so the undisturbed fluid will appear to be stationary. Only the streamwise velocity is considered as zero in Renard's formulation while there are no restrictions on the velocity in wall normal and spanwise directions. As the absolute reference frame moves at a constant speed, it is an inertial reference frame and so the pressure coincides in both the wall and absolute reference frames. Renard's formulation decomposes the generation of mean skin friction coefficient into a physical phenomenon at every local streamwise position and corresponding wall normal positions for a spatially developing flow. When seen from the absolute reference frame, C_f is represented as the mean power supplied to the fluid by the wall. C_{f_a} refers to the viscous dissipation. C_{f_c} can be interpreted as the mean streamwise kinetic energy gained by the fluid. In the absolute reference frame, Renard & Deck referred C_{f_b} as the dissipation because of production of turbulent kinetic energy [6]. Renard's formulation considers the contribution from the whole boundary layer profile. When seen from the absolute reference frame, the moving wall develops a non-zero power. In Renard's formulation, the Reynolds stress is weighted by the wall normal derivative of the mean streamwise velocity. This weight increases as we move closer to the wall as the velocity gradient increases towards the wall. Renard's formulation shows that in high Reynolds number ZPG TBL flows, the excess friction induced by turbulence is mostly located in the logarithmic layer [6].

Results and Discussion

Variation of C_f and its components with pressure gradient

The variation of skin friction coefficient calculated based on wall shear stress (C_{f_w}) and Renard's formulation (C_f) with pressure gradient can be seen in Figure 2.

Wall shear stress (τ_w) and C_{f_w} are defined as follows [5].

$$\tau_w = \mu \frac{d \langle u \rangle}{dy} \bigg|_{y=0} \tag{10}$$

$$C_{f_w} = \frac{\tau_w}{\frac{1}{2} \rho U_e^2} \tag{11}$$

C_f based on Renard's formulation and C_{f_w} are in close agreement with each other. As β varies from 0 to 39, C_f keeps reducing in Figure 2. With increasing pressure gradient, the boundary layer expands more rapidly in the wall-normal direction as it evolves in the streamwise direction. This reduces the mean velocity gradient at the wall which results in a reduction of skin friction coefficient with increasing pressure gradient. As the pressure gradient is increased, the flow becomes more like a free shear layer with the wall shear stress tending to zero.
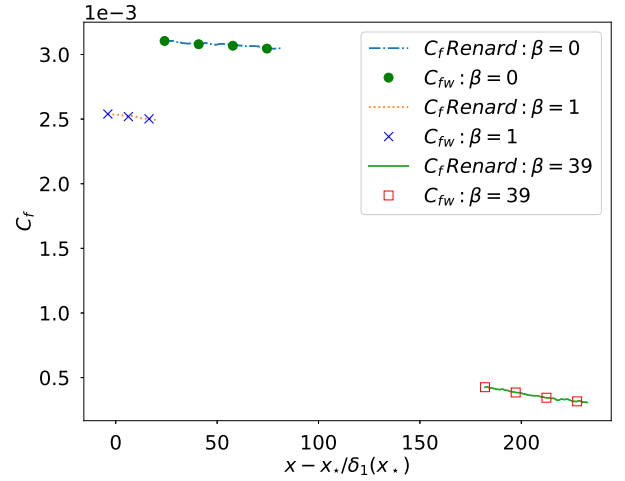
Figure 2: Variation of C_f based on Renard's formulation and C_{f_w} with β in the respective DoI. $x_\star$ is the streamwise position where $Re_{\delta_1} = 4800$.
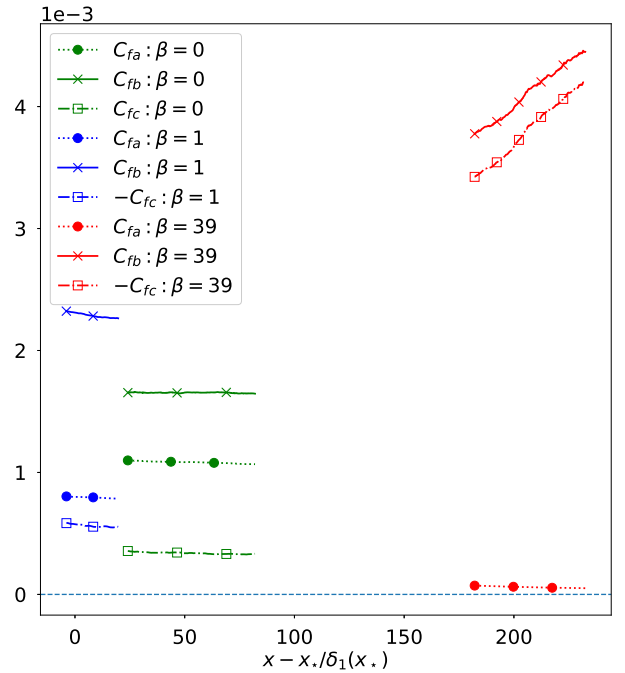
Figure 3: Variation of the components of C_f with β in the respective DoI. Note that C_{f_c} is negative for $\beta = 1$ and $\beta = 39$. $x_\star$ is the streamwise position where $Re_{\delta_1} = 4800$.

In the wall reference frame, C_{f_a} signifies the direct dissipation because of the viscous effects, C_{f_b} refers to the effect of turbulent fluctuations and C_{f_c} signifies the spatial growth in the flow. But when seen from the absolute reference frame, C_{f_c}/C_f is the efficiency at which the wall supplies energy to the fluid. C_{f_a} and C_{f_b} are positive for all pressure gradients. Note that C_{f_c} is positive only for ZPG case while it is negative for the other two adverse pressure gradient cases.

As β increases, the contribution of the viscous effects (C_{f_a}) reduces and approaches zero in Figure 3. With increase of β, the absolute values of C_{f_b} and C_{f_c} increases. It is also apparent that the absolute values of C_{f_b} and C_{f_c} develops with a sharp gradient in the streamwise direction for $\beta = 39$ when compared to the other two cases. The positive contribution to C_f by the turbulent fluctuations is diminished by the negative contribution from C_{f_c}. Still the dominant contribution to the skin friction coefficient for all the cases of β is from the Reynolds stress (C_{f_b}).
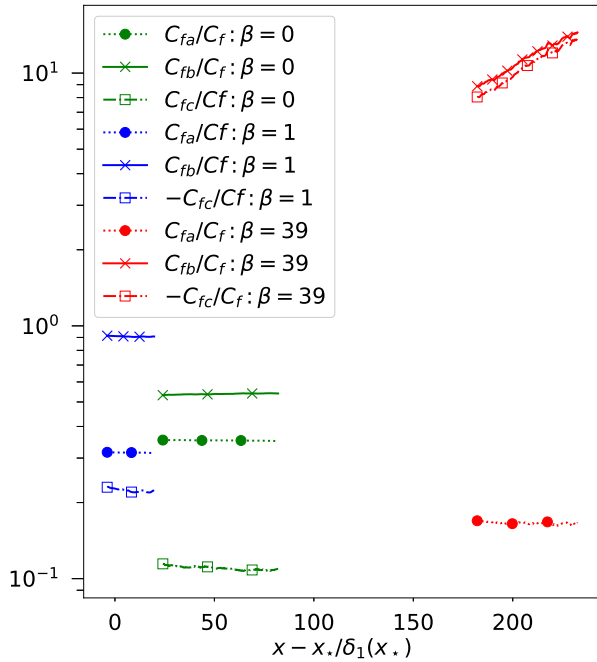
Figure 4: The variation of the proportion of each component in C_f with β in the respective DoI. Note that C_{f_c}/C_f is negative for $\beta = 1$ and $\beta = 39$. $x_\star$ is the streamwise position where $Re_{\delta_1} = 4800$.

The variation of the proportion of each component in C_f with β is seen in Figure 4. The proportion of the Reynolds stress (C_{f_b}/C_f) increases by 14 times when β varies from 0 to 39. The proportion of C_{f_b} and C_{f_c} increases drastically in the streamwise direction for $\beta = 39$ whereas they do not have steep gradients for $\beta = 0$ and $\beta = 1$. C_{f_c} acts to cancel out the effect of C_{f_b}. When closely observed, the proportion of C_{f_a} in C_f reduces with the pressure gradient. The ratio C_{f_a}/C_f is approximately 0.5 times smaller for $\beta = 39$ when compared to $\beta = 0$. The viscous dissipation accounts for 35% of C_f for $\beta = 0$ and its contribution drops down to 17.5% for $\beta = 39$.

Analysis of the premultiplied integrands

Figures 5, 6 and 8 show the streamwise averaged profiles of premultiplied integrand of each term of C_f in the wall-normal direction (y) within the DoI for various β. The wall normal position is non-dimensionalised by the outer scale δ_1. The

study based on the pre-multiplied integrands for a ZPG boundary layer flow is also discussed in detail in [2, 6]. Hereafter, the premultiplied integrand of each term of C_f is denoted by the subscript of *.

$$C_{fa*} = y \times \frac{2\nu}{U_e^3} \left(\frac{\partial \langle u \rangle}{\partial y} \right)^2 \quad (12)$$

$$C_{fb*} = y \times \frac{-2\langle u'v' \rangle}{U_e^3} \frac{\partial \langle u \rangle}{\partial y} \quad (13)$$

$$C_{fc*} = y \times \frac{2(\langle u \rangle - U_e)}{U_e^3} \frac{\partial}{\partial y} \left(\frac{\tau}{\rho} \right) \quad (14)$$

The viscous dissipation (C_{fa*}) exhibits an inner peak for the ZPG case in Figure 5. As the pressure gradient increases, the inner peak diminishes substantially while an outer peak develops for $\beta = 1$. The profile is almost uniform throughout the boundary layer for $\beta = 39$, with two similar tiny peaks in the inner and outer regions.
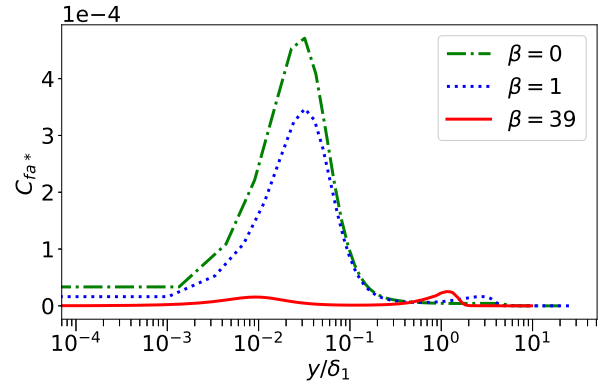
Figure 5: Variation of C_{fa} premultiplied integrand (C_{fa*}) with β. The profiles are averaged in streamwise direction within DoI and are non-dimensionalised by δ_1.

The variation of C_{fb*} and C_{fc*} with β is shown in Figure 6 and 8 respectively. The contribution of the turbulent fluctuations (C_{fb*}) has an inner peak and a outer peak for ZPG case as shown in Figure 6. As the pressure gradient increases, for $\beta = 1$, the inner peak reduces while the outer peak grows into a dominant one. For $\beta = 39$, the contribution from the Reynolds stress is almost negligible in the inner region and is concentrated in the outer region. $\beta = 39$ case has one predominant outer peak without any inner peak. Figure 7 shows the Reynolds stress profiles ($-\langle u'v' \rangle$) for all the pressure gradients. For $\beta = 39$, $-\langle u'v' \rangle$ has an outer peak at $y = \delta_1$ which matches with the peak of the C_{fb} premultiplied integrand (C_{fb*}) in Figure 6.

C_{fc*} in Figure 8 can be seen as the contribution of the pressure gradient. For ZPG case, its contribution is almost negligible throughout the boundary layer in the wall normal direction with a tiny peak in the outer region. As the pressure gradient increases, for $\beta = 1$, a negative and a positive peak start to develop in the outer region. These peaks are more pronounced and dominant for $\beta = 39$ with the inflection point at y = δ_1.
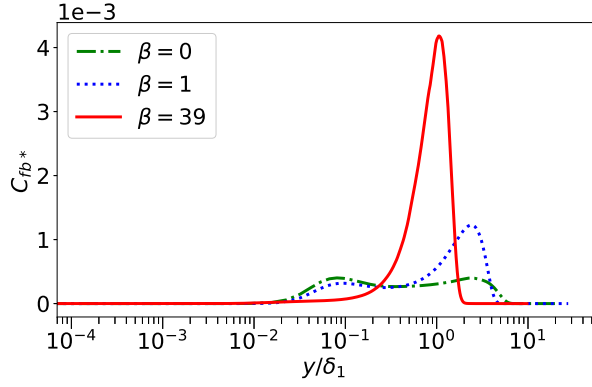
Figure 6: Variation of C_{f_b} premultiplied integrand ($C_{f_{b_*}}$) with β. The profiles are averaged in streamwise direction within DoI and are non-dimensionalised by δ_1.
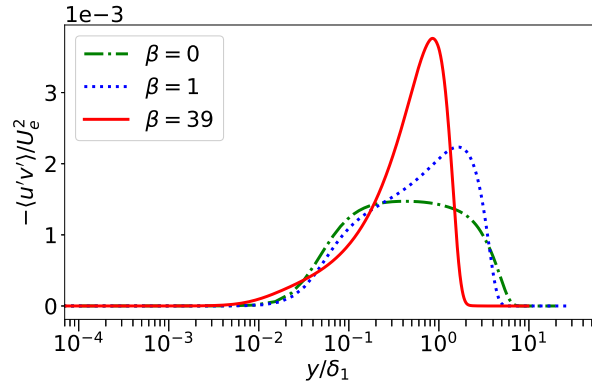
Figure 7: Variation of the Reynolds stress ($-\langle u'v' \rangle$) with β. The profiles are averaged in streamwise direction within DoI and are non-dimensionalised by δ_1 and U_e.
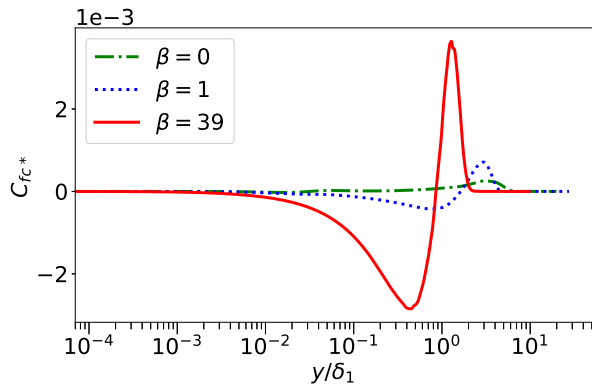
Figure 8: Variation of C_{f_c} premultiplied integrand ($C_{f_{c_*}}$) with β. The profiles are averaged in streamwise direction within DoI and are non-dimensionalised by δ_1.

Conclusions

With increasing pressure gradient, C_f approaches zero as the boundary layer expands more rapidly and the flow becomes more like a free shear layer (Figure 2). When β changes from 0 to 39, the Reynolds stress remains the dominant contribu-

tor while its effects are reduced by the negative contribution from C_{f_c} (Figure 3). The proportion of turbulent fluctuations (C_{f_b}/C_f) increases with a steep gradient along the streamwise direction for β = 39 (Figure 4). The contribution of viscous effects is 30% for β = 39 and it becomes half of it for β = 0. With increasing β, the distribution of viscous effects becomes more uniform in the wall normal direction (Figure 5) while the contribution of the Reynolds stress remains as the dominant factor with a clear outer peak at $y = \delta_1$ (Figure 6).

Acknowledgements

References

[1] Borrell, G., Sillero, J. A. and Jiménez, J., A code for direct numerical simulation of turbulent boundary layers at high Reynolds numbers in BG/P supercomputers, *Computers & Fluids*, **80**, 2013, 37–43.

[2] Deck, S., Renard, N., Laraufie, R. and Weiss, P.-É., Large-scale contribution to mean wall shear stress in high-Reynolds-number flat-plate boundary layers up to 13650, *Journal of Fluid Mechanics*, **743**, 2014, 202–248.

[3] Kitsios, V., Atkinson, C., Sillero, J. A., Borrell, G., Gungor, A. G., Jiménez, J. and Soria, J., Direct numerical simulation of a self-similar adverse pressure gradient turbulent boundary layer, *International Journal of Heat and Fluid Flow*, **61**, 2016, 129–136.

[4] Kitsios, V., Sekimoto, A., Atkinson, C., Sillero, J. A., Borrell, G., Gungor, A. G., Jiménez, J. and Soria, J., Direct numerical simulation of a self-similar adverse pressure gradient turbulent boundary layer at the verge of separation, *Journal of Fluid Mechanics*, **829**, 2017, 392–419.

[5] Pope, S. B., *Turbulent Flows*, Cambridge University Press, Cambridge, 2000.

[6] Renard, N. and Deck, S., A theoretical decomposition of mean skin friction generation into physical phenomena across the boundary layer, *Journal of Fluid Mechanics*, **790**, 2016, 339–367.

[7] Sillero, J. A., *High Reynolds number turbulent boundary layers*, Ph.D. thesis, Universidad Politénica de Madrid, 2014.

[8] Spalart, P. R. and Watmuff, J. H., Experimental and numerical study of a turbulent boundary layer with pressure gradients, *Journal of Fluid Mechanics*, **249**, 1993, 337–371.